

# Classification of Intervertebral Discs Using GLRLM Texture Features

Bazila Hashia,

*Department of Electronics and Communication Engineering, National Institute of Technology,  
Hazratbal, Srinagar 190006, India*

(E-mail: [samr\\_hashia@yahoo.co.in](mailto:samr_hashia@yahoo.co.in))

**Abstract**— Lower back pain is considered to be one of the major health issues in industrial countries. Statistics show that around 80% of the populations do have back pain at least once in their lifespan. A report from National Institute of Neurological Disorders and Stroke (NINDS) says that the growth rate of number of patients having back pain or some sort of intervertebral disk disorder is much higher than the growth rate of the radiologists. It is also reported that around 12 million MRI scans are done every year in USA alone on spine. The workload of radiologists has been increasing drastically over the years. In order to reduce the workload of radiologists there has been an increasing demand for computer aided diagnosis system. Computer aided diagnosis (CAD) system is one of the recent and major research areas in the sciences of medical imaging and radiology. In this paper texture analysis of MR images of intervertebral discs have been analyzed which can in turn help in developing a Computer aided diagnosis system for intervertebral disc disorders.

**Keywords**— *Intervertebral Discs, Texture analysis, MRI, GLRLM, SVM.*

## I. INTRODUCTION

Spine serves as crucial central axis for the musculoskeletal system and a soft defensive shell surrounding the most important neural pathway in the body, the spinal cord [1]. The capability of a human being to stand erect, bend, and twist is all possible because of the human spine. It is possible because human spine consists of almost all kinds of tissues, like, bones, cartilage, ligaments and muscles [2]. And if any kind of strain, injury or disease perturbs any of the parts of the spine, it causes severe pain.

A normal human spine in total has 33 vertebrae. The upper 24 are eloquent vertebrae and are separated by intervertebral discs, while the lower 9 are merged: five in the sacrum, and four in the coccyx. Intervertebral discs have 3 parts: (1) the nucleus pulposus classically described as a central gelatinous mass; (2) the annulus fibrosus, a fibrous outer ring; and (3) the vertebral end plate, constituting a cartilaginous layer covering the superior and inferior surfaces of the intervertebral disc [3]. There is no distinct demarcation between the nucleus pulposus and annulus fibrosus, and this area is sometimes referred to as the transitional zone. In intervertebral disc of young, healthy adults, the nucleus pulposus is a semifluid mass of mucoid material. Histologically, it consists of a few cartilage cells and

some irregularly arranged collagen - fibers, dispersed in a medium of semifluid ground substance. Biomechanically, the nucleus pulposus can deform under pressure but cannot be expanded or compressed. The annulus fibrosus surrounding the nucleus pulposus acts as a response to that pressure. The annulus fibrosus consists of collagen - fibers in a highly ordered pattern arranged in concentric rings[4].

Spine diseases being very common, affecting up to 80% of population worldwide, causing pain, disability and economic loss [5][6]. Back pain is considered to be the second highest health issue after common cold and is regarded as the second most common reason why patients visit doctors' clinic in USA and its global burden is estimated to increase distinctly in the next few decades, causing lot of disruption in peoples' lives, psychologically as well as economically [7][8][9][10]. Spine poses additional challenges to quantitative image analysis, because of its structure, as it consists of an array of vertebrae and discs, where the individual vertebrae and disc show complex shape, even the shape of the individual vertebrae and disc changes necessarily throughout the spine, mostly neighboring vertebrae and discs look very similar and are difficult to distinguish [11]. Such diversity brings challenges on multiple levels to the conventional vertebra and disc recognition and segmentation methods. For diagnosis and treatment of many spine related diseases, imaging is often required and different imaging modalities provide complementary information regarding both anatomy and physiology.

Aging, trauma, genetic disorders, nutritional disorders usually result in the change in the gross anatomy, ultrastructure, and boundaries of these regions, resulting in the degeneration of the intervertebral discs [12].

In this paper we have used GLRLM texture analysis for classifying MR images of normal and degenerated intervertebral discs.

In section II literature review is discussed, in section III Methodology and in section IV Implementation and in section V results and discussion then in section VI Conclusion.

## II. EASE OF USE

Mir et al. [13] have used Spatial Grey Level Dependence Matrix (SGLDM), Grey Level Run Length Matrix (GLRLM), Grey Level Difference Matrix (GLDM) for detection of abnormalities in CT images that are beyond visual perception. Wang et al. [14] have utilized texture features based on First

Order Statistics (FOS), spatial gray level dependence matrix (SGLDM), gray level run length matrix (GLRLM) and gray level difference matrix (GLDM) for classification of hepatic tissues from CT images. Kim et al. [15] have used SGLDM, GLRLM, GLDM, for the detection of microcalcifications in digitized mammograms. Vince et al. [16] have used five different texture analysis techniques, namely: first order statistics, Haralick’s method, Laws’ texture energy method, the neighborhood grey–tone difference matrix, and texture spectrum features, on intravascular ultrasound images and concluded that GLCM method gave much more satisfying results. Gibbs et al. [17] have used GLCM texture features and have concluded that there are momentous differences between benign and malignant lesions in the breast MRI. Valavanis et al. [18] used SGLDM and GLDM for retrieving texture features to classify hepatic tissue non-enhanced CT images into four classes. Guillermo et al. [19] have used GLCM, GLDM and GLRLM techniques for classification of abdominal aortic aneurysm after endovascular repair. Claudia et al. [20] have exploited statistical and spectral texture features for automatic segmentation of intervertebral discs of scoliotic spines from MRI. Khawla et al. [21] explored GLCM for detection of abnormalities in MR images of spine. Ghosh et al. [22] have proposed fully automated lumbar herniation diagnosis system on MR images. Intensity and texture features have been generated and fed into five different classifiers and have taken majority voting scheme into consideration and have achieved 94.85% accuracy, 95.9% specificity and 92.45% sensitivity for 35 clinical cases.

In this study the capacity of GLRLM for the classification of degenerated intervertebral disc and normal disc is analyzed. For this Region of Interest (ROI) is extracted. The features of the extracted ROI are fed into SVM classifier for automatic classification.

III. METHODOLOGY

A. Region of interest (ROI)

It is very important to know the exact region of which the features are to be extracted, which is called as the region of interest (ROI). In the selection of ROI, one has to balance between the need to capture appropriate textural information for classification purposes with the desire to avoid multiple tissue categories [23]. The method used for determining the ROI in medical images is still an active research area. The method used can be either manual or automatic [24]. Selection of ROI not only helps in fast and efficient processing but also minimizes noise and artifacts and hence in increasing diagnostic accuracy [25].

B. Feature Extraction Using GLRLM

GLRLM is a matrix from which we can extract higher order statistical texture features. In GLRLM we define run length as maximal set of pixels having same grey level. In this matrix the grey level runs are described by the grey level of the run, the length of the run and the direction of the run. For a given image, GLRLM is a two-dimensional matrix in which each element  $x(i, j/\theta)$  represents the total number of runs with pixels of grey value  $i$ , ( $0 \leq i \leq Ng$ ,  $Ng$  is the utmost grey level) and run length  $j$  ( $0 \leq j \leq Rmax$ ,  $Rmax$  is the maximum length) in a

certain direction  $\theta$  ( $0^\circ, 45^\circ, 90^\circ$  &  $135^\circ$ ). Therefore, in a given direction, run length matrix measures how many times there are runs of, for example, 2 or 3 or 4 consecutive pixels with the same value for each acceptable grey level value, and hence for each direction many different run length matrices can be computed for a single image. The number of the grey levels is minimized by re-quantization before the build-up of the matrix [26][27].

Figure 1(a) below shows a matrix of size 4\*4 pixel image with 4 gray values and Figure 1(b) is the representation matrix GLRL (gray level run length) in the direction of  $0^\circ$  [ $x(i, j/\theta=0^\circ)$ ].

1	2	3	4
1	3	4	4
3	2	2	2
4	1	4	1

Figure 1 a) 4\*4 Matrix of Image

GREY LEVE L (i)	RUN LENGTH (j)			
	1	2	3	4
1	4	0	0	0
2	1	0	1	0
3	3	0	0	0
4	3	1	0	0

Figure 1 b) GLRL Matrix

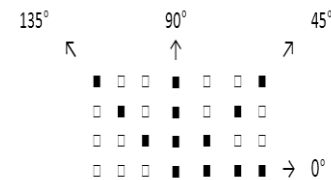


Figure 2 Run Direction

The Gray Level Run Length Matrix (GLRLM) was initially developed by Galloway in 1975 [27] and suggested 5 texture features based on GLRLM namely: Shot Runs Emphasis (SRE), Long Runs Emphasis (LRE), Gray Level Non-uniformity (GLN), Run Length Non-Uniformity (RLN), and Run Percentage (RP). Chu et al. added two more features called Low Gray Level Run Emphasis (LGRE) and High Gray Level Run Emphasis (HGRE) and later Asarathy and Holder added 4 more features extracted from the GLRLM, namely: Short Run Low Gray-Level Emphasis (SRLGE), Short Run High Gray-Level Emphasis (SRHGE), Long Run Low Gray-Level Emphasis (LRLGE), and Long Run High Gray-Level Emphasis (LRLGE).

C. Classification Using SVM

SVM is a state-of-art classifier initially introduced by Boser et al. [28] in the year 1992 for binary classification. The basic concept of SVM is to develop a hyper-plane that helps in defining the boundaries used in the decision making of the classification. And with this concept of hyper-plane SVMs are able to deal with both linearly separable data as well non separable data (nonlinear) in simple as well as complex classification assignments. In SVM the original data points are mapped from the input space to a high dimensional feature space. The mapping is done using a kernel function [29]. For

this reason SVM tends to generalize better [5]. With the basic design of Support Vector Machines, it can only discriminate between two classes. Support Vector Machines in their simple form, are called linear classifiers. It is possible however to create a nonlinear SVM by increasing the dimensionality of the feature space, and by using the so-called "kernel-trick". It is thus possible to find a separating hyper plane in a higher dimensions where such a hyper plane would not exist in lower dimensions. There are many choices for which kernel, to use. The standard choices are the linear kernel (which is otherwise called as dot-product kernel), the polynomial kernel and the Gaussian Kernel. The Gaussian Kernel is the special case of Radial Basis Function (RBF) kernel [30]. In the standard case, the distance used, is the Euclidean distance. In the RBF kernel, the parameters determine, the width of the kernel, and  $d(x, y)$  is the distance metric. RBF is a reasonable first choice among other Kernels due to its generality and computational efficiency [31]. We have used LS-SVM [32].

IV. IMPLEMENTATION

A. Database

The dataset used contains clinical MRI scans of 99 symptomatic patients having back pain, 12000 numbers of scans, and almost 4800 to 6000 numbers of discs, and these images are mostly from lumbar region of the spine, few are from thoracic and cervical region as well. The patients being examined demonstrate number of radiologically defined abnormalities, but in this thesis only disc herniation is being studied and diagnosed. The MR images of 99 patients/cases used for evaluation range from age group of 16 to 78 years. MEDICARE, a private diagnostic center at Srinagar, India has provided the data set used. The MR images provided by MEDICARE were in DICOM format, having matrix resolution mostly of 240\*240 and 256\*205, slice thickness ranging from 1.7 mm to 6 mm and slice gap ranging from 20 to 300 percent, TR ranging from 3.3 milliseconds to 7.8 milliseconds and TE ranging from 1.27 milliseconds to 3.69 milliseconds and flip angle ranging from 8 degrees to 20 degrees. The simulation platform used is MATLAB 2010.

B. Selection of the ROI

In this study the ROI is manually selected. First and foremost slice analysis is done, in which the proper slice that gives almost all the details about the structure for characterization and diagnosis is selected. For disc herniation diagnosis mid-sagittal, T2- weighted slices are being used [5] [33]. The ROI in this work is limited to the region that includes the interface of the vertebrae, intervertebral disc and that of spinal cord and the size of the ROI is a window of 33x33 pixels.

C. Feature extraction using GLRLM

In this study all the eleven GLRLM features have been extracted and they are mentioned in table 1.

Feature	Formula
Short Run Emphasis	$SRE = 1/n_r \sum_{i=1}^{Ng} \sum_{j=1}^{Rmax} x(i, j) / j^2$
Long Run Emphasis	$LRE = 1/n_r \sum_{i=1}^{Ng} \sum_{j=1}^{Rmax} x(i, j) * j^2$
Grey-Level Non-uniformity	$GLN = 1/n_r \sum_{i=1}^{Ng} [\sum_{j=1}^{Rmax} x(i, j)]^2$
Run Length Non-uniformity	$RLN = 1/n_r \sum_{j=1}^{Rmax} [\sum_{i=1}^{Ng} x(i, j)]^2$
Run Percentage	$RP = \frac{nr}{x(i,j)*j}$
Low Grey-Level Run Emphasis	$LGRE = 1/n_r \sum_{i=1}^{Ng} \sum_{j=1}^{Rmax} x(i, j) / i^2$
High Grey-Level Run Emphasis	$HGRE = 1/n_r \sum_{i=1}^{Ng} \sum_{j=1}^{Rmax} x(i, j) * i^2$
Short Run Low Grey-Level Emphasis	$SRLGE = 1/n_r \sum_{i=1}^{Ng} \sum_{j=1}^{Rmax} x(i, j) / (i^2 * j^2)$
Short Run High Grey-Level Emphasis	$SRHGE = 1/n_r \sum_{i=1}^{Ng} \sum_{j=1}^{Rmax} x(i, j) * i^2 / j^2$
Long Run Low Grey-Level Emphasis	$LRLGE = 1/n_r \sum_{i=1}^{Ng} \sum_{j=1}^{Rmax} x(i, j) * j^2 / i^2$
Long Run High Grey-Level Emphasis	$LRHGE = 1/n_r \sum_{i=1}^{Ng} \sum_{j=1}^{Rmax} x(i, j) * (i^2 * j^2)$

Table 1 Eleven features of GLRLM Matrix

The size of the feature vector extracted from GLRLM is 44D, from 11 GLRLM features evaluated initially along just one direction and that is 0°, and then along 4 directions with inter-pixel distance of 1 (in this thesis all the features have been calculated at a distance of 1 due to reduced size of the samples) and out of 11 features only 3 features namely, Gray-Level Non-uniformity (GLN), High Gray-Level Run Emphasis (HGRE), Long Run High Gray-Level Emphasis (LRHGE) along 4 directions have been used for classification, making feature vector dimension equal to 12D (Figure 3).

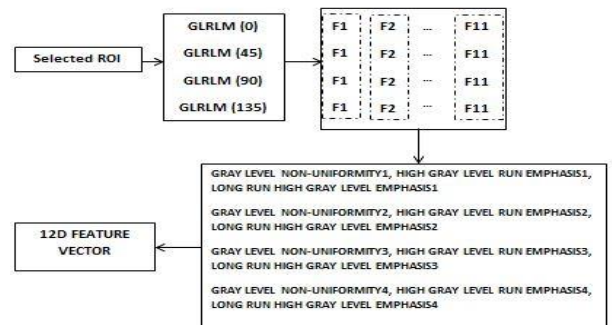


Figure 3. Selection of the Feature vector from GLRLM

The 12D GLRLM feature vector is fed to SVM classifier as shown in the figure 4.

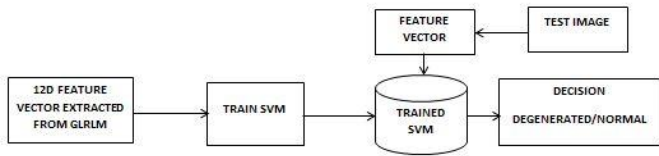


Figure 4.12D GLRLM Feature Vector fed to SVM

V. RESULTS AND DISCUSSION

A. Performance Parameters used

i) Accuracy:

The accuracy of a test is its ability to differentiate the patient and healthy cases correctly. To estimate the accuracy of a test, we should calculate the proportion of true positive and true negative in all evaluated cases. Mathematically, this can be stated as:

$$\text{Accuracy} = (TP+TN)/(TP+TN+FP+FN)$$

ii) Specificity:

The specificity of a test is its ability to determine the healthy cases correctly. To estimate it, we should calculate the proportion of true negative in healthy cases. Mathematically, this can be stated as:

$$\text{Specificity} = TN/(TN+FP)$$

iii) Sensitivity

The sensitivity of a test is its ability to determine the patient cases correctly. To estimate it, we should calculate the proportion of true positive in patient cases. Mathematically, this can be stated as:

$$\text{Sensitivity} = TP/(TP+FN)$$

Where TP is true positive rate, TN is true negative rate, FP is false positive rate and FN is false negative rate.

Experimental results are presented in order to validate the discussed methodology and the performance of the methodology is evaluated on the discussed database.

The table 2 illustrates Average and Standard Deviation and the Confidence Interval at 95% of confidence level, extracted from the selected features of GLRLM.

Features	Normal IVD			Abnormal IVD		
	Average	Standard deviation	CI	Average	Standard deviation	CI
Direction = 0°, Distance = 1						
Gray-Level Non-uniformity (GLN)	43.5987 6	21.0156 9	36.2660 50.9315	39.9675 2	14.8925 3	34.7713 45.1638
High Gray-Level Run Emphasis (HGRE)	71.7011 6	37.5513 9	58.5989 84.8035	73.9697 8	40.7879	59.7382 88.2014
Long Run High Gray-	390.289 7	147.160 4	338.943 0	324.362 9	134.110 2	277.569 6

Level Emphasis (LRHGE)			441.636 4			371.156 2
Direction = 45°, Distance = 1						
Gray-Level Non-uniformity (GLN)	93.2103 5	41.3960 4	78.7666 107.654 1	69.3925 1	23.3777 5	61.2356 77.5494
High Gray-Level Run Emphasis (HGRE)	20.1263 1	9.50775 4	16.8089 23.4437	29.3093	13.9707 4	24.4347 34.1839
Long Run High Gray-Level Emphasis (LRHGE)	112.864 3	33.7668 3	101.082 5 124.646 1	125.650 1	50.9695	107.866 0 143.434 2
Direction = 90°, Distance = 1						
Gray-Level Non-uniformity (GLN)	56.3050 7	29.2149 4	46.1115 66.4986	43.1525 4	19.8852 2	36.2143 50.0908
High Gray-Level Run Emphasis (HGRE)	32.7140 4	14.3287	27.7145 37.7136	39.1334 7	18.0334 1	32.8413 45.4256
Long Run High Gray-Level Emphasis (LRHGE)	177.443 3	43.4053 8	162.298 4 192.588 2	173.252 4	57.6287 7	153.144 8 193.360 0
Direction = 135°, Distance = 1						
Gray-Level Non-uniformity (GLN)			83.6875 111.1817			62.5667 80.6482
High Gray-Level Run Emphasis (HGRE)	18.41801	7.973935	15.6358 21.2002	71.60749	25.91095	18.9124 25.2423
Long Run High Gray-Level Emphasis (LRHGE)	104.1605	27.8056	94.4587 113.8623	98.91255	28.85089	88.8460 108.9791

Table 2 Tabulated average and standard deviation feature values for normal IVD and abnormal IVD extracted from GLRLM

The GLRLM features fed to the classifier were selected on the basis of the values of average, standard

deviation and the Confidence Interval at 95% of confidence level.

It is obvious from the table 2 that the values of the average, standard deviation and Confidence Interval of both the normal and the abnormal classes are overlapping and the classification cannot be performed linearly.

In this study we have used Receiver Operating Characteristic graph, i.e. ROC, as it has very extensive assessment capacity (r). ROC is a graph between sensitivity and 1-specificity, i.e. true positive fraction (TPF) as a function of false positive fraction.

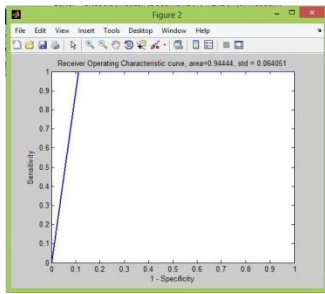


Figure 5 a) ROC plot for GLRLM along four directions

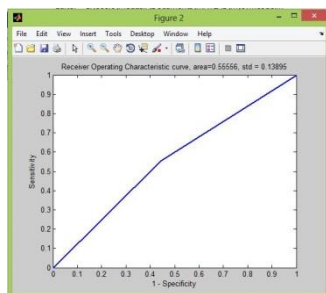


Figure 5 b) ROC plot for GLRLM along one directions

The accuracy, specificity and sensitivity values are given in the table 3 below.

TEXTURE FEATURES EXTRACTED	DIRECTION	SVM		
		ACC	SPEC	SEN
GLRLM (3 features)	0°	0.555	0.555	0.555
GLRLM (3 features)	0°, 45°, 90°, 135°	<b>0.8333</b>	<b>1</b>	<b>0.666</b>

Table 3 Accuracy, specificity and sensitivity values

In disc degeneration diagnosis, specificity is of more importance than sensitivity, i.e. the rate at which the cases without diseases are identified is of more importance than the rate of the diseased cases, and otherwise the patient may undergo unnecessary treatment procedure.

VI. CONCLUSION

In this study, I have analyzed the discriminative capability of GLRLM texture features for classifying normal

intervertebral disc and degenerated intervertebral disc. Only three features selected on the bases of the average, standard deviation and the Confidence Interval at 95% of confidence level where fed to SVM classifier. The results obtained allow us to assert that the normal intervertebral discs and degenerated intervertebral discs correspond to different texture parameters.

REFERENCES

- [1] J. Okamoto and T. Women, “CARS 2015 — Computer Assisted Radiology and Surgery Proceedings of the 29th International Congress and Exhibition,” vol. 10, 2015.
- [2] J. Women, H. Care, and A. P. Sumchai, “Journal of Women ’ s Health Care The Human Spine is like a Precious Strand of Pearls,” vol. 4, no. 5, pp. 1–8, 2015.
- [3] W. C. W. Chan, K. L. Sze, D. Samartzis, V. Y. L. Leung, and D. Chan, “S t r u c t u r e a n d B i o l o g y of the Intervertebral Disk in Health and Disease,” *Orthop. Clin. NA*, vol. 42, no. 4, pp. 447–464.
- [4] “Anatomy of the Spine,” pp. 2–6.
- [5] J. Koh, V. Chaudhary, and G. Dhillon, “Diagnosis of disc herniation based on classifiers and features generated from spine MR images,” *Spie Med. Imaging Comput. Aided Diagnosis*, vol. 7624, no. June, p. 762430–762430–8, 2010.
- [6] J. K. Freburger *et al.*, “NIH Public Access,” vol. 169, no. 3, pp. 251–258, 2015.
- [7] Arthritis Research UK, “State of Musculoskeletal Health 2017,” *Arthritisresearchuk.Org*, p. 30, 2017.
- [8] L. Manchikanti, V. Singh, S. Datta, S. P. Cohen, and J. a Hirsch, “Comprehensive review of epidemiology, scope, and impact of spinal pain.,” *Pain Physician*, vol. 12, no. 4, pp. E35–E70, 2009.
- [9] R. S. Alomari, J. J. Corso, and V. Chaudhary, “Labeling of lumbar discs using both pixel- and object-level features with a two-level probabilistic model,” *IEEE Trans. Med. Imaging*, vol. 30, no. 1, pp. 1–10, 2011.
- [10] K. Alawneh, M. Al-dwiekat, M. Alsmirat, and M. Al-Ayyoub, “Computer-aided diagnosis of lumbar disc herniation,” *2015 6th Int. Conf. Inf. Commun. Syst.*, pp. 286–291, 2015.
- [11] D. Board, B. D. Stemper, N. Yoganandan, F. A. Pintar, B. Shender, and G. Paskoff, *Biomechanics of the aging spine*, vol. 42, no. May. 2006.
- [12] S. K. Michopoulou, L. Costaridou, E. Panagiotopoulos, R. Speller, G. Panayiotakis, and A. Todd-Pokropek, “Atlas-based segmentation of degenerated lumbar intervertebral discs from MR images of the spine,” *IEEE Trans. Biomed. Eng.*, vol. 56, no. 9, pp. 2225–2231, 2009.
- [13] I. Engineering, B. Magazine, M. National, and T. Delhi, “Texture Analysis of CT Images,” no. April 2016, 1995.
- [14] L. Wang *et al.*, “Classification of Hepatic Tissues from CT

- Images Based on Texture Features and Multiclass Support Vector Machines,” pp. 374–381, 2009.
- [15] J. K. Kim and H. W. Park, “Statistical textural features for detection of microcalcifications in digitized mammograms,” *IEEE Trans. Med. Imaging*, vol. 18, no. 3, pp. 231–238, 1999.
- [16] D. G. Vince, K. J. Dixon, R. M. Cothren, and J. F. Cornhill, “Comparison of texture analysis methods for the characterization of coronary plaques in intravascular ultrasound images,” *Comput. Med. Imaging Graph.*, vol. 24, no. 4, pp. 221–9, 2000.
- [17] P. Gibbs and L. W. Turnbull, “Textural analysis of contrast-enhanced MR images of the breast,” *Magn. Reson. Med.*, vol. 50, no. 1, pp. 92–98, 2003.
- [18] I. K. Valavanis, S. G. Mougiakakou, A. Nikita, and K. S. Nikita, “Evaluation of texture features in hepatic tissue characterization from non-enhanced CT images,” *Annu. Int. Conf. IEEE Eng. Med. Biol. - Proc.*, pp. 3741–3744, 2007.
- [19] G. García, J. Maiora, A. Tapia, and M. De Blas, “Evaluation of texture for classification of abdominal aortic aneurysm after endovascular repair,” *J. Digit. Imaging*, vol. 25, no. 3, pp. 369–376, 2012.
- [20] C. Chevfrefils, F. Chériet, G. Grimard, and C.-E. Aubin, “Watershed Segmentation of Intervertebral Disk and Spinal Canal from MRI Images,” *Image Anal. Recognit.*, vol. 4633, no. 3, pp. 1017–1027, 2007.
- [21] K. H. Ali, E. B. Tala, and N. J. Alsaad, “Co-occurrence Matrix for a Spine MRI Images,” vol. 14, no. 9, pp. 666–670, 2016.
- [22] S. Ghosh, R. S. Alomari, V. Chaudhary, and G. Dhillon, “Computer-aided diagnosis for lumbar mri using heterogeneous classifiers,” *Proc. - Int. Symp. Biomed. Imaging*, pp. 1179–1182, 2011.
- [23] M. Sikiö, L. Harrison, and H. Eskola, “The Effect of Region of Interest Size on Textural Parameters A study with clinical magnetic resonance images and artificial noise images,” no. Ispa, pp. 149–153, 2015.
- [24] R. Janaki, “Enhanced ROI ( Region of Interest Algorithms ) for Medical Image Compression,” vol. 38, no. 2, pp. 38–43, 2012.
- [25] J. Koh, V. Chaudhary, and G. Dhillon, “Disc herniation diagnosis in MRI using a CAD framework and a two-level classifier,” *Int. J. Comput. Assist. Radiol. Surg.*, vol. 7, no. 6, pp. 861–869, 2012.
- [26] V. A. N. Gool, “Texture Analysis Anno 1983,” 1985.
- [27] M. M. Galloway, “Texture analysis using gray level run lengths,” *Comput. Graph. Image Process.*, vol. 4, no. 2, pp. 172–179, 1975.
- [28] B. E. Boser, I. M. Guyon, and V. N. Vapnik, “A Training Algorithm for Optimal Margin Classifiers,” *Proc. fifth Annu. Work. Comput. Learn. theory*, pp. 144–152, 1992.
- [29] R. Palaniappan, K. Sundaraj, and S. Sundaraj, “A comparative study of the svm and k-nn machine learning algorithms for the diagnosis of respiratory pathologies using pulmonary acoustic signals,” *BMC Bioinformatics*, vol. 15, no. 1, pp. 1–8, 2014.
- [30] G. Charpiat, M. Hofmann, and B. Sch, “Kernel Methods in Medical Imaging,” pp. 1–18.
- [31] I. El-naqa *et al.*, “for Detection of Microcalcifications,” vol. 21, no. 12, pp. 1552–1563, 2002.
- [32] L. Lalaoui, T. Mohamadi, and M. Chemachema, “Support Vector Machine ( SVM ) and the Neural Networks for Segmentation the Magnetic Resonance Imaging,” pp. 1–5, 2009.
- [33] J. Koh, P. D. Scott, V. Chaudhary, and G. Dhillon, “An automatic segmentation method of the spinal canal from clinical MR images based on an attention model and an active contour model,” *Biomed. Imaging From Nano to Macro, 2011 IEEE Int. Symp.*, pp. 1467–1471, 2011.



Bazila Hashia has received her BE in Electronics and Communication Engineering from University of Kashmir, India and then received her MTech from NIT Srinagar in the year 2010. And has worked as lecturer in the department of Electronics and Communication from Aug 2010 to Dec 2012. Presently she is a research scholar at NIT Srinagar in the department of Electronics and Communication. Her areas of interest are Biometrics, Image processing, patter recognition.